Pergamon

Int. J. Solids Structures Vol. 33, No. 1, pp. 79–97, 1996

0020-7683/96 $9.50 + .00

0020-7683(95)00019-4

ON SAINT-VENANT'S PRINCIPLE IN PIN-JOINTED FRAMEWORKS

N. G. STEPHEN and P. J. WANG†
Department of Mechanical Engineering, The University, Southampton SO17 1BJ, U.K.

(*Received* 25 *March* 1994; *in revised form* 5 *January* 1995)

Abstract—Numerical experiments performed by Hoff 50 years ago on the application of Saint-Venant's principle to frameworks are extended, and his conclusions qualified. Guided by these results, a general treatment is formulated employing a state variable approach; this leads directly to an eigenvalue problem in which the decay rates are the eigenvalues of the cell transfer matrix. Unity eigenvalues correspond to the transmitting modes of rigid body displacement and the stress resultants of tension, bending moment, shearing force and twisting moment. Consideration of the associated eigenvectors and principal vectors gives exact values for the equivalent "continuum" beam properties of the framework, such as equivalent cross-sectional area, Poisson's ratio, second moment of area, shear coefficient and torsion constant.

1. INTRODUCTION

Saint-Venant's principle (SVP) underpins much of solid mechanics by allowing the replacement of an actual load system on a structural member by a statically equivalent load distributed in a particular way demanded by the elastostatic solution; the difference between the two load distributions is termed "self-equilibrating", and since it has no stress resultant or couple which requires reaction at some other location on the structure, there seems no reason why the associated stress field should penetrate any great distance into the structure. According to SVP this depth of penetration should be small.

SVP has been expressed and applied in a variety of ways by many authors; for example in beam problems, according to Sokolnikoff (1956), "it is commonly assumed that the local eccentricities are not felt at distances that are about five times the greatest linear dimension of the area over which the forces are distributed".

The first mathematical proof of SVP was provided by Toupin (1965), who considered an elastic cylinder of arbitrary length and cross-section subjected to a self-equilibrated load system on one end only; Toupin demonstrated the exponential decay of elastic strain energy, and hence stress, but SVP requires also that the rate of decay should be "rapid". In practice there are many examples, particularly for thin-walled structural members, where the rate of exponential decay is so slow that SVP cannot really be said to apply. One example is the effect of (self-equilibrated) longitudinal warping restraint during torsion, when it is necessary to introduce the *bimoment* (Vlasov, 1961), in order to provide a plausible engineering theory.

The vast majority of published results pertaining to SVP [see recent reviews by Horgan and Knowles (1983) and Horgan (1989)] have concentrated on *continuum* structural members, including isotropic, anisotropic and composite structures. One of the earliest studies of SVP by Hoff (1945) considered application to aircraft structures and demonstrated this slow decay in thin-walled structures; to explain, Hoff performed various "numerical experiments" with space frameworks (i.e. a three-dimensional pin-jointed truss) for which exact analysis was possible, albeit laborious.

In the present paper we first re-examine the numerical experiments conducted by Hoff and qualify his conclusions; with the ready availability of computer programs for structural analysis, this is now a simple task. In preparation for a general treatment, further numerical experiments are conducted on various plane frameworks which, while simple, disallow

† Visiting Research Fellow from the Department of Mechanical Engineering, Shanghai Maritime Institute, Shanghai 200135, People's Republic of China

torsional and out of plane loadings. As with Hoff, the purpose of this investigation included the further elucidation of factors which may affect decay within a continuum structure (where exact elasticity solutions are only available for mathematically amenable cross-sections such as the circle or plane strain strip), but with the increased interest in large flexible space frameworks for astronautical application such a study is of interest in its own right. Pin-jointed frameworks are traditionally analysed by calculation of the tensile or compressive load in each member, requiring consideration of the whole framework, although there are techniques which allow consideration of a single or group of members. However, it can be advantageous to estimate the overall structural performance of a framework prior to such detailed analysis, for which a "continuum" beam model is useful. Such models have been constructed by Renton (1984) and Noor and co-workers by a variety of means including energy and finite difference methods; a review of this approach was presented by Noor (1988).

SVP and the beam-like behaviour of a framework are closely related in two ways: firstly, as Renton (1984) has observed, it is the validity of SVP which permits the approximate analysis of a space framework using a continuum "beam" model. Secondly, unless one knows the required distribution of nodal forces which constitutes a transmitting resultant—for example, a bending moment or axial force—then it may be impossible to know what is a decaying mode; in effect, one wishes to know the framework equivalent of $\sigma_x = My/I$, and $\sigma_x = F/A$ for the stress distribution due to bending and tension. For a continuum model one requires equivalent values for second moment of area I and cross-sectional area A. For a framework consisting of a series of identical repeated cells, Renton employed a finite difference technique wherein the displacements of adjacent nodal sections are related by a finite difference operator; the transmitting modes have deflection functions which are finite polynomials of the cell number, while the decaying modes are typified by deflections showing piecewise oscillatory decay.

The general treatment developed here employs a transfer matrix to relate the vector of state variables—the nodal displacement and forces—on either side of a generic cell; the transfer matrix may be readily determined from a knowledge of the cell stiffness matrix. Guided by the numerical experiments it is recognized that the state vector at any nodal section will be a constant multiple (λ) of the state vector at the previous section; this leads immediately to an eigenvalue problem. The decaying eigenvalues are (generally) distinct, occurring in reciprocal pairs; the transmitting eigenvalue ($\lambda = 1$) has a multiplicity of six for the two-dimensional framework (12 for the three-dimensional) and eigenvectors for rigid body translations are coupled with principal vectors describing rigid body rotation and the transmitting resultants, that is tension, shear, bending moment and torsion for the three-dimensional case. The matrix of eigenvectors and principal vectors then forms a similarity matrix which transforms the original transfer matrix into Jordan canonical form, indicating that the transfer matrix is both defective and derogatory.

Bi-orthogonality properties of the eigenvectors then allow modal decomposition of an arbitrary end load. A detailed examination of the coupling between the transmitting eigenvectors and the associated principal vectors gives exact values for the continuum beam properties of the framework, such as equivalent cross-sectional area, Poisson's ratio, second moment of area, shear coefficient and, for the three-dimensional framework, the torsion constant.

The procedure is developed fully in conjunction with a two-dimensional example, and finally applied to one of Hoff's three-dimensional frameworks.

2. HOFF'S NUMERICAL EXPERIMENTS

Hoff first analysed a statically determinate four cell framework subjected to a "warping group" of four axial forces of magnitude 100 applied at one end, as shown in Fig. 1; the force group is self-equilibrated, having no resultant tension or bending moment, and may be described as a bimoment. This framework was subsequently modified by the addition of new (redundant) members, when the analysis was repeated.

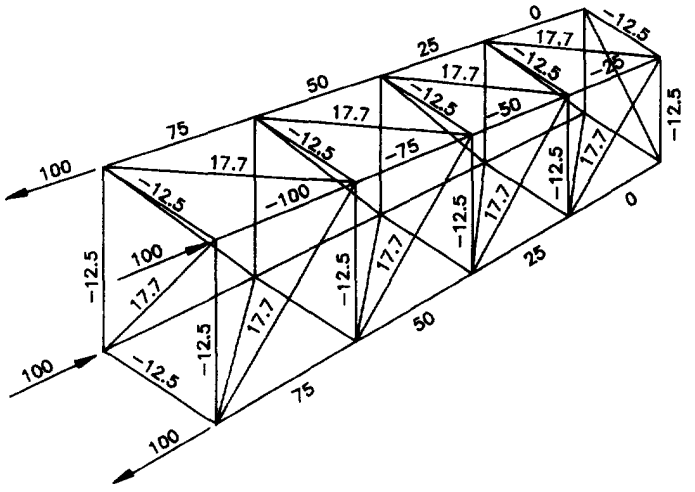

Fig. 1. Statically determinate framework considered by Hoff (his Fig. 6).

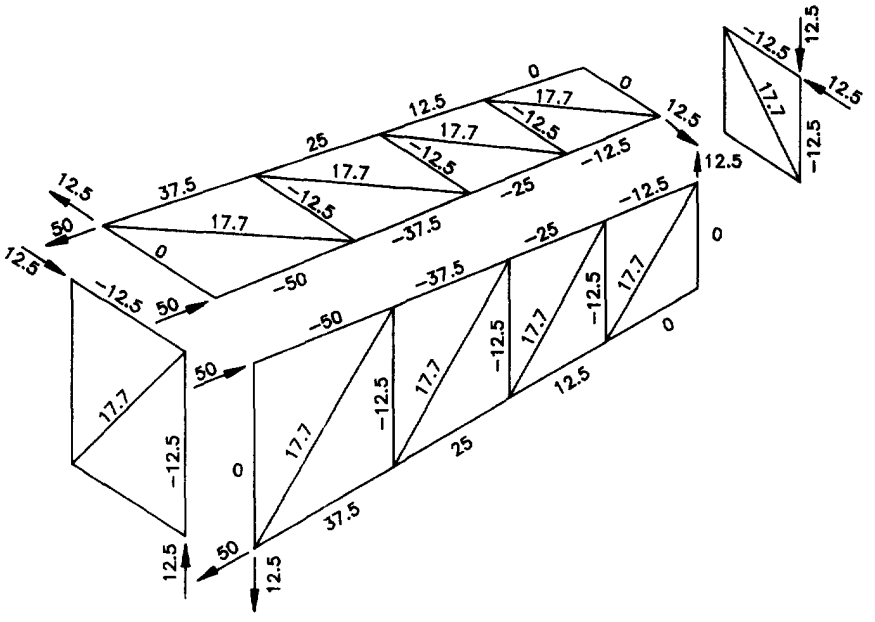

Fig. 2. Decomposition of framework in Fig. 1; member forces and reactions from lower and rear faces not shown.

For the statically determinate framework, Hoff noted that the maximum force in the end (fourth) cell is still noticeable, having reduced to 25% of the applied load, but argued that since only one state of equilibrium is possible in a statically determinate framework, SVP can hardly be expected to apply. Hoff did not note that the majority of the member forces are constant, while the axial members showing a linear force variation from cell to cell. In terms of equivalent "beam" behaviour of one side of the framework this is consistent with a constant shearing force and linear variation of bending moment: thus the longitudinal member force may reduce to zero over four cells precisely because there are four cells! This equivalent "beam" behaviour can be seen when the three-dimensional truss is decomposed† into the six two-dimensional statically determinate trusses which are the "faces" and "ends" of the space framework (Fig. 2). Thus when Hoff's framework is extended to 10 cells then, consistent with linear variation, these longitudinal forces are reduced to zero over 10 cells.

† This decomposition is only possible because of the absence of internal or transverse diagonals within each cell.

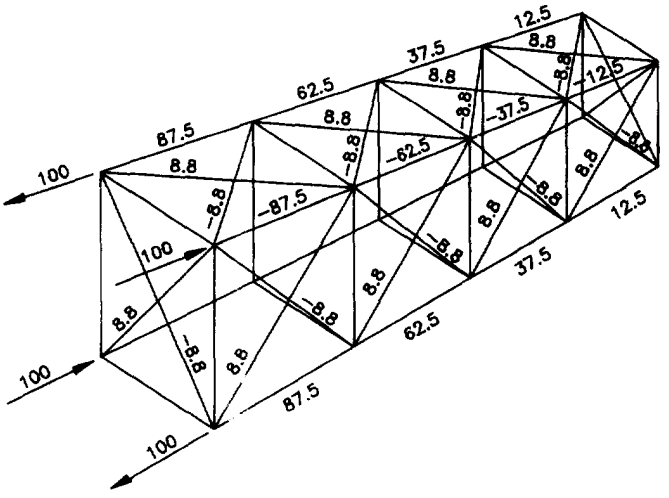

Fig. 3. Statically indeterminate framework considered by Hoff (his Fig. 7); 18 redundant bars.

Hoff then modified this four cell framework by the addition of a second diagonal to the face of each cell (Fig. 3), expecting that SVP would be fully applicable by virtue of the high degree of redundancy. According to Hoff, "This anticipation, however, is only partially fulfilled, since the maximum load in the fourth field is still 12.5% of the value of the load applied to one corner. The redistribution of the load consists only in evening out the differences between the forces acting in adjacent flanges of the same bay." Again Hoff failed to note the constant/linear variation of member forces, and again it is possible to decompose this framework into six two-dimensional trusses in order to see this equivalent beam behaviour. In fact the SVP decay is completely absent, and the "evening out" of longitudinal member forces is attributable to the "face" symmetry of this second framework; thus the longitudinal member forces in the fourth cell of Fig. 1 are zero and -25, while the equivalent members in Fig. 3 have ± 12.5.

Finally, Hoff added further transverse diagonals to the three inner "bulkheads" (Fig. 4), and noted that the addition of the six new redundant bars "is extremely effective in localizing the internal forces in the structure", when the applied load was reduced to a maximum 0.7% in the fourth cell. Inspection of the bar forces along the framework does not readily indicate the character of the variation, other than it is neither linear nor exponential; this example will be considered further in a later section, when it will become

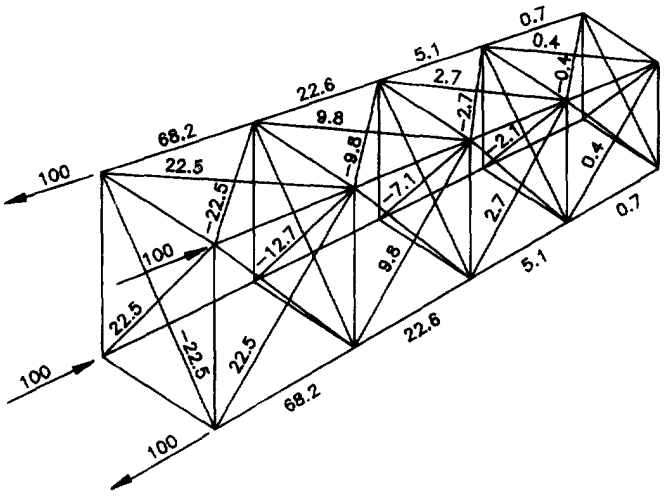

Fig. 4. Statically indeterminate framework considered by Hoff (his Fig. 8); 24 redundant bars.

apparent that only for this last framework can the decay anticipated by SVP be seen in action.

The conclusions drawn by Hoff from his numerical experiments were:

(1) The principle of SVP can be applied to the case of a redundant framework.

(2) If the plane of loading is braced, the tendency towards the equalization of strains is pronounced, and the distance required for the variation of strains to become negligible is dependent to a great extent upon the efficiency of the bracing in this and parallel planes.

The first of these conclusions is true as far as it goes, but Hoff's second framework shows that redundancy does not guarantee the applicability of SVP; on the other hand it will be seen that non-zero member forces for a self-equilibrating end load applied to a statically determinate framework may be confined to at most one cell, with all other members transmitting zero force, when SVP is clearly applicable. The second conclusion requires qualification: without bracing in the end plane of loading and at the free end, both of Hoff's first two frameworks become mechanisms; extra bracing in the faces does tend to equalize load, but only in the sense of equalizing force distribution within one cell; variation from cell to cell is completely unaltered, remaining constant or linear variation. What does make SVP applicable is the additional "bulkhead" bracing in planes parallel to the end face, as in Fig. 4.

3. SOME FURTHER NUMERICAL EXPERIMENTS

Structural analyses were performed using either ANSYS 4.4A on a SUN workstation, or GJMAS† on an IBM PC. All frameworks considered have the following bar properties: Young's modulus $E = 200 \times 10^9$ N m^{-2}, length $L = 1$ m, diagonal bars have length $\sqrt{2}$ m, horizontal and vertical bars have cross-sectional area $A = 1$ cm^2, while diagonal bars have cross-sectional area $A\sqrt{2}$; these proportions are the same as those employed by Hoff.

3.1. *Statically determinate example*

Hoff suggested that one could hardly expect SVP to be applicable to a statically determinate framework as only one state of equilibrium is possible; this should be re-stated as one state of equilibrium *for each applied load.*

Thus consider the simple two-dimensional statically determinate "K" truss shown in Fig. 5; by superposition we see that the self-equilibrated difference between applying a compressive end load of magnitude 200 at the central pin joint rather than equally distributed over the two outer joints will decay over the first cell. Thus SVP can be applied to a statically determinate framework.

On the other hand, it is possible to construct a statically determinate framework, as in Figs 6(a,b), where the member forces due to a self-equilibrated load are transmitted without decay (rather they are oscillatory) until a stable sub-structure is reached.

3.2. *Two-dimensional statically indeterminate frameworks*

The operation of SVP in frameworks can be adequately described, and more clearly seen, by restricting attention to two-dimensional frameworks. Inspection of Fig. 7 shows that, with the exception of the first loaded cell, the member force in each adjacent cell is reduced by a constant factor of approximately 0.517 as one moves away from the loaded end; this is the framework equivalent of exponential decay. Denoting the ratio of member forces **B** in the $(j-1)$th and jth cells as λ, an equivalent exponential decay rate may be determined as

† GJMAS is a general purpose finite element package developed in the People's Republic of China to run on a PC under the Microsoft operating system.

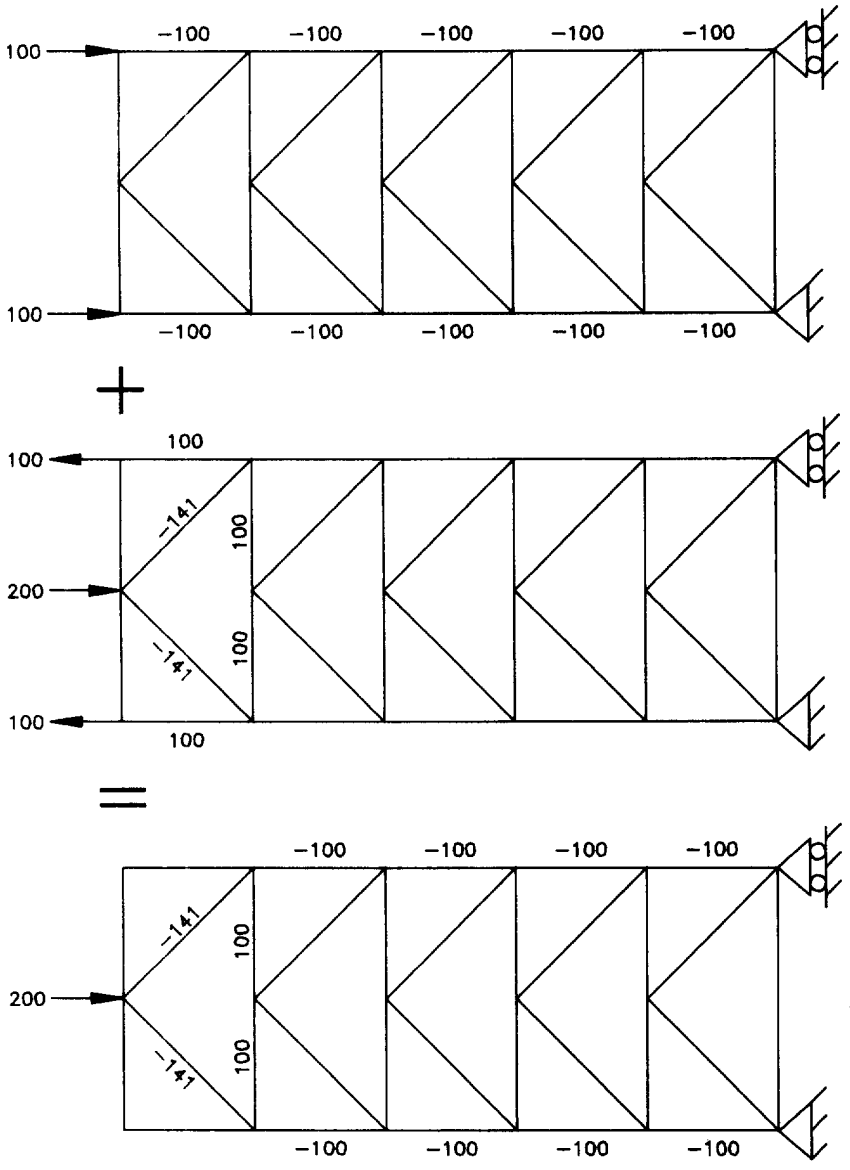

Fig. 5. Superposition of end loads for statically determinate two-dimensional framework showing application of Saint-Venant's principle; self-equilibrated load decays over one cell.

$$\lambda = \frac{\mathbf{B}_{j+1}}{\mathbf{B}_j} = \frac{\mathbf{B}_0 \, e^{k(j+1)}}{\mathbf{B}_0 \, e^{kj}} = e^k, \quad k = \ln(\lambda). \tag{1}$$

For the truss in Fig. 7, $k = -0.66$.

We now modify the framework by the addition of further diagonal members (Fig. 8), again these have a cross-sectional area one half that of the horizontal and vertical members. Inspection of the bar forces shows that, as with Hoff's example (Fig. 3), decay is not by a constant factor although it does approach the constant value $\lambda = 0.2829$, equivalent to $k = -1.263$. Also it is seen that addition of these new diagonals has resulted in more rapid decay.

In both these examples, the bar force decay characteristic is as the sum of two or more exponential decay modes; in the first example (Fig. 7), one mode decays completely over the first cell, leaving a single exponential decay. In the second, this modal decomposition cannot be seen by inspection and a more general theoretical treatment is required.

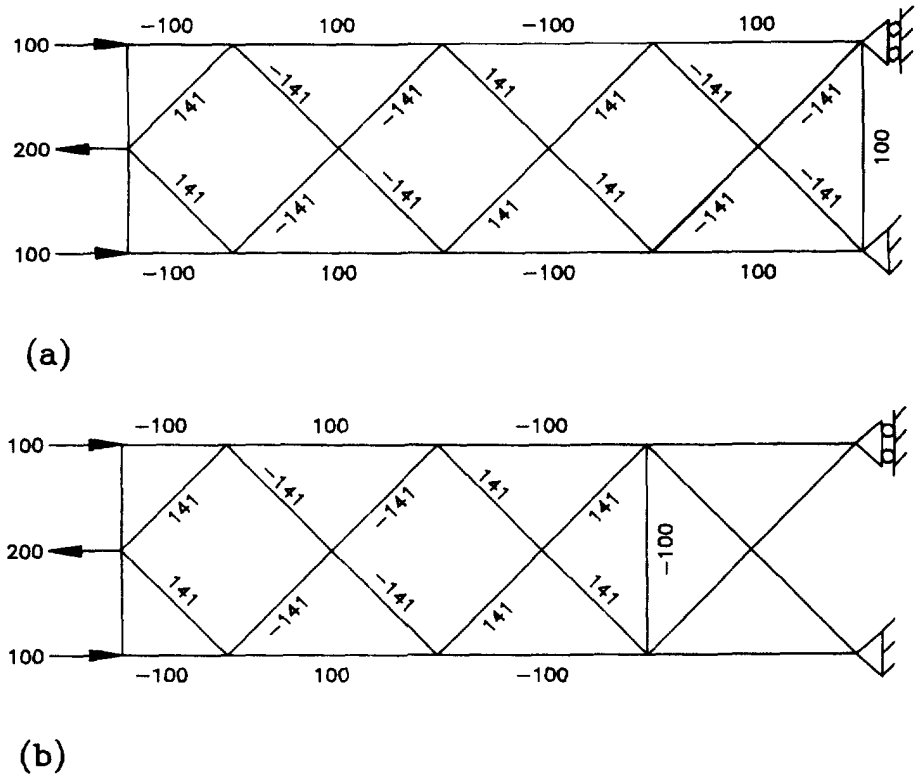

Fig. 6. Statically determinate frameworks with oscillatory member forces.

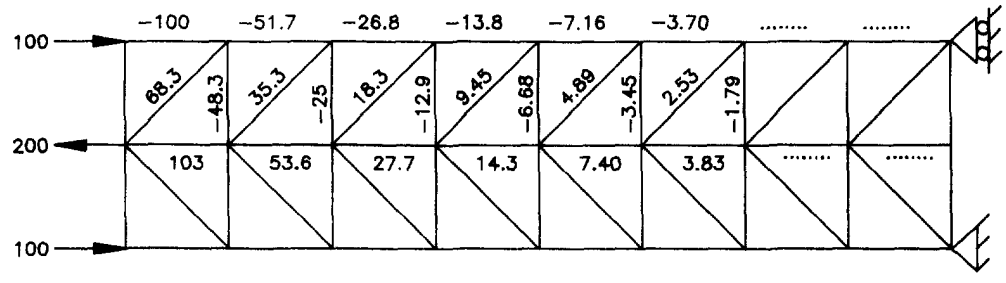

Fig. 7. Two-dimensional statically indeterminate framework ; member forces are symmetric. Decay factor $\lambda = 0.517$, $k = -0.660$.

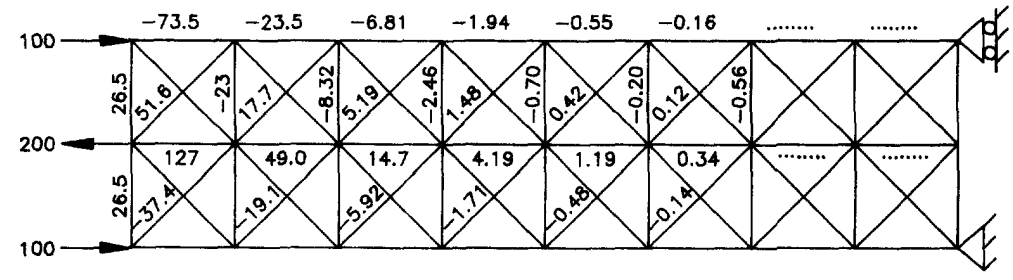

Fig. 8. Two-dimensional statically indeterminate framework ; member forces are symmetric. Decay factor λ approaches $\lambda = 0.2829$, $k = -1.263$.

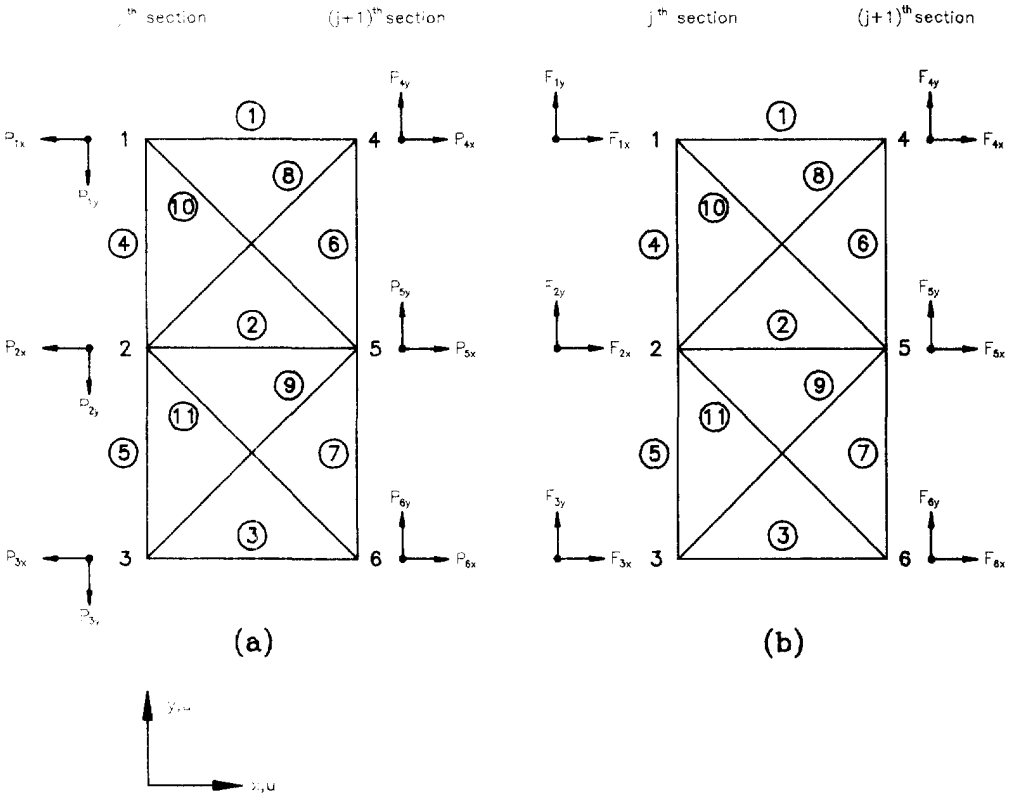

Fig. 9. Single (jth) cell of framework in Fig. 8; (a) and (b) show, respectively, positive joint loads according to transfer matrix and finite element methods.

4. TRANSFER MATRIX METHOD

Consider the jth cell located between the jth and $(j+1)$th sections of the two-dimensional framework in Fig. 8, as shown in Fig. 9(a). Let $\mathbf{p}_j$ and $\mathbf{d}_j$ denote the nodal force and displacement vectors* respectively, associated with the jth section; the state vectors at the sections j and $(j+1)$ are then $\mathbf{s}_j = [\mathbf{d}_j \mathbf{p}_j]^T$ and $\mathbf{s}_{j+1} = [\mathbf{d}_{j+1} \mathbf{p}_{j+1}]^T$. State vectors on either side of the cell are related by the transfer matrix $\mathbf{G}$ through the equation

$$\mathbf{s}_{j+1} = \mathbf{G}\mathbf{s}_j \tag{2}$$

or in partitioned form

$$\begin{bmatrix} \mathbf{d}_{j+1} \\ \mathbf{p}_{j+1} \end{bmatrix} = \begin{bmatrix} \mathbf{G}_{dd} & \mathbf{G}_{dp} \\ \mathbf{G}_{pd} & \mathbf{G}_{pp} \end{bmatrix} \begin{bmatrix} \mathbf{d}_j \\ \mathbf{p}_j \end{bmatrix}. \tag{3}$$

Now from our numerical experiments, particularly the two-dimensional framework of Fig. 7, where the applied end load is clearly self-equilibrating, it was seen that member forces $\mathbf{B}$ decayed by a constant factor λ from cell to cell. Consideration of Hooke's law would suggest that the nodal displacements associated with this self-equilibrated load should also decay in similar manner, and we therefore set

$$\mathbf{s}_{j+1} = \lambda \mathbf{s}_j. \tag{4}$$

Substituting the above into eqn (2) gives

* Positive forces are defined according to the conventions of the Theory of Elasticity.

$$\lambda \mathbf{s}_j = \mathbf{G}\mathbf{s}_j, \quad [\mathbf{G} - \lambda \mathbf{I}]\mathbf{s}_j = 0. \tag{5}$$

Thus the decay factors λ are the eigenvalues of the transfer matrix $\mathbf{G}$; the associated eigenvectors give the jth section nodal displacements and loads for the particular decay mode. One simple method of obtaining the transfer matrix of the cell is from its stiffness matrix $\mathbf{K}$; referring to Fig. 9(b), the force and displacement vectors, $\mathbf{F}$ and $\mathbf{d}$, are related by the matrix equation $\mathbf{F} = \mathbf{K}\mathbf{d}$, where

$$\begin{bmatrix} \mathbf{F}_j \\ \mathbf{F}_{j+1} \end{bmatrix} = \begin{bmatrix} \mathbf{K}_{j,j} & \mathbf{K}_{j,j+1} \\ \mathbf{K}_{j+1,j} & \mathbf{K}_{j+1,j+1} \end{bmatrix} \begin{bmatrix} \mathbf{d}_j \\ \mathbf{d}_{j+1} \end{bmatrix}; \tag{6}$$

because, by convention, the force vector $\mathbf{F}$ is defined positive when the components are parallel to the coordinate directions, we have $\mathbf{F}_j = -\mathbf{p}_j$, $\mathbf{F}_{j+1} = \mathbf{p}_{j+1}$, and substituting into eqn (6), expanding and rearranging gives

$$\begin{bmatrix} \mathbf{d}_{j+1} \\ \mathbf{p}_{j+1} \end{bmatrix} = \begin{bmatrix} \mathbf{K}_{j,j+1}^{-1}\mathbf{K}_{j,j} & -\mathbf{K}_{j,j+1}^{-1} \\ \mathbf{K}_{j+1,j} - \mathbf{K}_{j+1,j+1}\mathbf{K}_{j,j+1}^{-1}\mathbf{K}_{j,j} & -\mathbf{K}_{j+1,j+1}\mathbf{K}_{j,j+1}^{-1} \end{bmatrix} \begin{bmatrix} \mathbf{d}_j \\ \mathbf{p}_j \end{bmatrix}. \tag{7}$$

Note that the stiffness matrix $\mathbf{K}$ is symmetric, but will be singular as the cell is not fixed in any way.

5. TWO DIMENSIONAL EXAMPLE

We continue with the two-dimensional framework shown in Fig. 8; the force and displacement vectors are, from Fig. 9(a),

$$\begin{aligned} \mathbf{p}_j &= [P_{1x}\ P_{1y}\ P_{3x}\ P_{2x}\ P_{3y}\ P_{2y}]^{\mathrm{T}} \\ \mathbf{p}_{j+1} &= [P_{4x}\ P_{4y}\ P_{5x}\ P_{5y}\ P_{6y}\ P_{6x}]^{\mathrm{T}} \\ \mathbf{d}_j &= [v_1\ v_1\ u_2\ v_2\ u_3\ v_3]^{\mathrm{T}} \\ \mathbf{d}_{j+1} &= [v_4\ v_4\ u_5\ v_5\ u_6\ v_6]^{\mathrm{T}}. \end{aligned} \tag{8}$$

The cell stiffness matrix $\mathbf{K}$ can be determined by the finite element method [see, for example, Stasa (1985)], or by matrix structural analysis [see, for example, Przemieniecki (1968)], but for brevity is not presented here. Matrix manipulations were performed using MATLAB to give the eigenvalues and eigenvectors. The eigenvalues are

$$\begin{bmatrix} 16.7798 \\ 0.0596 \end{bmatrix}, \begin{bmatrix} 3.5346 \\ 0.2829 \end{bmatrix}, \begin{bmatrix} 14.2435 \\ -0.0702 \end{bmatrix},$$

occurring as three reciprocal pairs, as might be expected, together with six unity eigenvalues associated with "rigid body" translational and rotational displacements of the cross-sectional plane, and nodal forces having a cross-sectional resultant which are therefore transmitted along the framework.

We consider first the decaying modes: if λ is an eigenvalue, then so is $1/\lambda$ and the equivalent decay rates are then $k = \ln(\lambda)$, and $-k = \ln(1/\lambda)$. The "slowest" decay factor (eigenvalue) pair is $[3.5346\ 0.2829]^{\mathrm{T}}$, and a self-equilibrated load on the left face of the cell reduces in magnitude by a factor 0.2829 as one moves to the right face,† i.e.

† In dynamics the duration of a temporal exponential decay $\exp(-t/\tau)$ is often taken as the time for it to reduce to less than 2% of its initial value, and this is normally taken as four time constants (4τ); in the present problem the spatial decay $\exp(-1.263)$ reduces to 2.3% over three cells, and to 0.64% over four cells.

$$\mathbf{p}_{j+1} = 0.2829\mathbf{p}_j, \quad \text{or} \quad \mathbf{p}_{j+1} = \mathbf{p}_j e^{-1.263}.$$

On the other hand, suppose the self-equilibrated load is applied to the right face of the cell: the magnitude is again reduced by the same factor, 0.2829, as one moves to the left face, i.e.

$$\mathbf{p}_j = 0.2829\mathbf{p}_{j+1},$$

but as one transfers across the cell from left to right according to the transfer matrix formulation, the load *increases*, i.e

$$\mathbf{p}_{j-1} = 3.5346\mathbf{p}_j, \quad \text{or} \quad \mathbf{p}_{j-1} = \mathbf{p}_j e^{1.263}.$$

This slowest decay rate is the one observed in the "numerical" experiment (Fig. 8) after the more rapid modes have decayed.

The second "slowest" decay factor is $\lambda = 0.0596$, $k = -2.8201$, and the third is $\lambda = -0.0702$, $k = -2.6564 + \pi i$; the negative eigenvalue indicates that the bar forces change sign from cell to cell, which is oscillatory decay. The eigenvectors associated with each of these decay eigenvalues are given in the Appendix, and the nodal forces are shown in Fig. 10.

If we now return to our second numerical experiment, Fig. 8, we see that the applied end load $\mathbf{p}_0$ consists of two decay modes

$$\begin{bmatrix} 100 \\ 0 \\ -200 \\ 0 \\ 100 \\ 0 \end{bmatrix} = \alpha_4 \begin{bmatrix} 100 \\ -243.5 \\ -200 \\ 0 \\ 100 \\ 243.5 \end{bmatrix} + \alpha_5 \begin{bmatrix} 100 \\ -78 \\ -200 \\ 0 \\ 100 \\ 78 \end{bmatrix}, \tag{9}$$

where, by simple calculation, $\alpha_4 = -0.4713$, $\alpha_5 = 1.4713$. Nodal forces at the nth section† may then be determined from the equation

$$\begin{bmatrix} P_{1x} \\ P_{1y} \\ P_{2x} \\ P_{2y} \\ P_{3x} \\ P_{3y} \end{bmatrix} = -0.4713 \begin{bmatrix} 100 \\ -243.5 \\ -200 \\ 0 \\ 100 \\ 243.5 \end{bmatrix} 0.0596^n + 1.4713 \begin{bmatrix} 100 \\ -78 \\ -200 \\ 0 \\ 100 \\ 78 \end{bmatrix} 0.2829^n \tag{10}$$

and member forces within the cell can then be calculated from a knowledge of the nodal forces on the nth and $n+1$th sections.

Alternatively this self-equilibrating end load may be expanded into its constituent decay modes by employing the bi-orthogonality property of the eigenvectors. Denoting the ith and jth eigenvectors of the transfer matrix $\mathbf{G}$ and its transpose $\mathbf{G}^T$ as $\mathbf{X}_i$ and $\mathbf{Y}_j$, repectively, then, as is well known

$$(\lambda_i - \lambda_j)\mathbf{Y}_j^T\mathbf{X}_i = 0, \tag{11}$$

and hence the bi-orthogonality property $\mathbf{Y}_j^T\mathbf{X}_i = 0$ when $\lambda_i \neq \lambda_j$; in the event of independent eigenvectors having the same eigenvalue, as occurs in the three-dimensional example, the above leads to a simple algebraic calculation.

† It is assumed that the load is applied on the end section $n = 0$.

If we now denote the *applied* end state vector as $\mathbf{s}_0$, and expand as

$$\mathbf{s}_0 = \sum_{i=1}^{m} \alpha_i \mathbf{X}_i, \tag{12}$$

where m is the number of eigenvectors, then pre-multiplying by $\mathbf{Y}_j^{\mathrm{T}}$ gives

$$\mathbf{Y}_j^{\mathrm{T}}\mathbf{s}_0 = \sum_{i=1}^{m} \alpha_i \mathbf{Y}_j^{\mathrm{T}}\mathbf{X}_i = \alpha_j \mathbf{Y}_j^{\mathrm{T}}\mathbf{X}_j,$$

and hence

$$\alpha_j = \frac{\mathbf{Y}_j^{\mathrm{T}}\mathbf{s}_0}{\mathbf{Y}_j^{\mathrm{T}}\mathbf{X}_j}. \tag{13}$$

This general procedure cannot yet be implemented: although the applied load is known, the displacement components are not; that is $\mathbf{s}_0 = [\mathbf{d}_0\ \mathbf{p}_0]^{\mathrm{T}}$, and thus far only $\mathbf{p}_0$ is known. The required vector $\mathbf{d}_0$ may be determined from the boundary conditions at the right-hand end of the framework which we suppose is fixed. The state vector at the nth nodal section is related to the free (left-hand) end state vector $\mathbf{s}_0$ by

$$\begin{bmatrix}\mathbf{d}_n\\ \mathbf{p}_n\end{bmatrix} = \mathbf{G}^n \begin{bmatrix}\mathbf{d}_0\\ \mathbf{p}_0\end{bmatrix}. \tag{14}$$

Strictly the framework should be of semi-infinite length, when $\mathbf{d}_n \to 0$ as $n \to \infty$; however, from the numerical point of view the larger n, the greater the errors introduced into $\mathbf{G}^n$. In this example the slowest decay rate has $\lambda = 0.2829$, when $\lambda^6 = 0.00051$, $\lambda^8 = 0.000041$, and we take the later as negligible in relation to unity. We therefore set

$$\begin{bmatrix}\mathbf{d}_8\\ \mathbf{p}_8\end{bmatrix} = \mathbf{G}^8 \begin{bmatrix}\mathbf{d}_0\\ \mathbf{p}_0\end{bmatrix} = \begin{bmatrix}0\\ 0\end{bmatrix}, \quad \text{or} \quad \begin{bmatrix}\mathbf{A} & \mathbf{B}\\ \mathbf{C} & \mathbf{D}\end{bmatrix}\begin{bmatrix}\mathbf{d}_0\\ \mathbf{p}_0\end{bmatrix} = \begin{bmatrix}0\\ 0\end{bmatrix},$$

where **A**, **B**, **C** and **D** are the partitioned sub-matrices of $\mathbf{G}^8$. Then

$$\mathbf{A}\mathbf{d}_0 + \mathbf{B}\mathbf{p}_0 = 0, \quad \mathbf{d}_0 = -\mathbf{A}^{-1}\mathbf{B}\mathbf{p}_0.$$

We now expand the free end state vector as†

$$\mathbf{s}_0 = \sum_{i=1}^{6} \alpha_i \mathbf{X}_i$$

and employing eqn (13) gives the coefficients as

$$\alpha_1 = O(-9), \quad \alpha_2 = O(-8), \quad \alpha_3 = -\alpha_6 = O(-7), \quad \alpha_4 = -0.4712, \quad \alpha_5 = 1.4712,$$

which agree with our previous result. [O is order (of magnitude).]

We now turn to the eigenvectors associated with the unity eigenvalues, i.e. the transmission modes; MATLAB employs a QR algorithm which returns a transformation matrix of 12 independent eigenvectors which *will* diagonalize the original transfer matrix. The

† Although there are 12 eigenvectors, we exclude those pertaining to rigid body displacements, since $\mathbf{d}_8 = 0$, and also the transmission mode eigenvectors pertaining to the resultants, as the applied end load is clearly self-equilibrating. We include both the "left to right" and "right to left" decay modes in order to illustrate that there is no contribution from the latter.

computed eigenvalues are close to, but not exactly, unity; however, by physical argument they must be exactly unity and this is imposed by solving the set of equations†

$$(\mathbf{G}-\mathbf{I})\mathbf{X}_i = 0, \tag{15}$$

where $\mathbf{I}$ is the identity matrix, employing the reduced row echelon form command "RREF" within MATLAB. This shows that there are only two independent eigenvectors associated with $\lambda = 1$, which are the rigid body displacement in the x- and y-directions. The procedure for obtaining the principal vectors ($\mathbf{Z}_i$) is to set up the chain of equations

$$\begin{aligned} \mathbf{G}\mathbf{X}_i &= \mathbf{X}_i \\ \mathbf{G}\mathbf{Z}_1 &= \mathbf{Z}_1 + \mathbf{X}_i \\ \mathbf{G}\mathbf{Z}_2 &= \mathbf{Z}_2 + \mathbf{Z}_1, \text{etc.} \end{aligned} \tag{16}$$

and again use the RREF command on the augmented matrix $[\mathbf{G}-\mathbf{I}, \mathbf{X}_i]$ to find $\mathbf{Z}_1$, etc. In this way it is found that the "beam" resultant of tension is coupled with rigid body displacement in the x-direction, and shearing force is coupled to bending moment, which in turn is coupled to rotational displacement and thence rigid body displacement in the y-direction. The complete similarity or transformation matrix of eigenvectors and principal vectors is given in the Appendix together with the Jordan canonical form of the transfer matrix.

The coupled eigenvectors and principal vectors associated with the unity eigenvalues allow determination of the equivalent "beam" properties of the framework. Thus consider the seventh and eighth columns of the transformation matrix $\mathbf{T}$ (Appendix) which give rise to the 2×2 Jordan block: we use the MATLAB syntax to identify these columns as $\mathbf{T}(:, 7)$ and $\mathbf{T}(:, 8)$, respectively. The rigid body displacement in the x-direction, $\mathbf{T}(:, 7)$, is the eigenvector and can exist in its own right if the cell, or indeed the framework, is not restrained: more importantly it is the "generating" eigenvector for the principal vector defining tension, according to the chain of equations (16). Thus for these vectors we have

$$\mathbf{G}\mathbf{T}(:, 8) = \mathbf{T}(:, 8) + \mathbf{T}(:, 7). \tag{17}$$

This representation is shown physically in Fig. 11, where we see that a total tensile load of $T = 1 + 2 \times 0.89645 = 2.7929$, is coupled with a cell elongation of 3.9645×10^{-8}. For a continuum beam the constitutive relationship is

$$T = AE\frac{\delta u}{L}, \tag{18}$$

and in this example, $AE/L = 2 \times 10^5$, to give an equivalent cross-sectional area of 3.522386 cm^2, which represents the sum of each axial bar cross-sectional area (which is three) plus a contribution from the diagonal members. Additionally there is a "Poisson's ratio" contraction of the cross-section: strain in the x-direction, $\varepsilon_x = \delta u/L = 3.9645 \times 10^{-8}$, while strain in the y-direction, $\varepsilon_y = (-2 \times 1.0355 \times 10^{-8})/2 = -1.0355 \times 10^{-8}$, and writing $\varepsilon_y = -\nu\varepsilon_x$ we find the equivalent Poisson's ratio $\nu = 0.2612$.

The ninth to twelfth columns of the transformation matrix are coupled within a 4×4 Jordan block associated with shear and bending stress resultants, and cross-sectional rotation and transverse displacements. Again a rigid body displacement, now in the y-direction, $\mathbf{T}(:, 9)$, is the eigenvector and can exist in its own right if the cell or framework is not restrained. The tenth column, $\mathbf{T}(:, 10)$, defines a rigid body rotation of the cell and this is coupled with the transverse displacement of the cell according to

† For numerical reasons it was found necessary to reduce temporarily the value of Young's modulus by two orders of magnitude to $E = 200 \times 10^7$ N m^{-2} whilst using the "RREF" routine within MATLAB, thereby increasing the magnitude of the displacements, making them less susceptible to computational error.

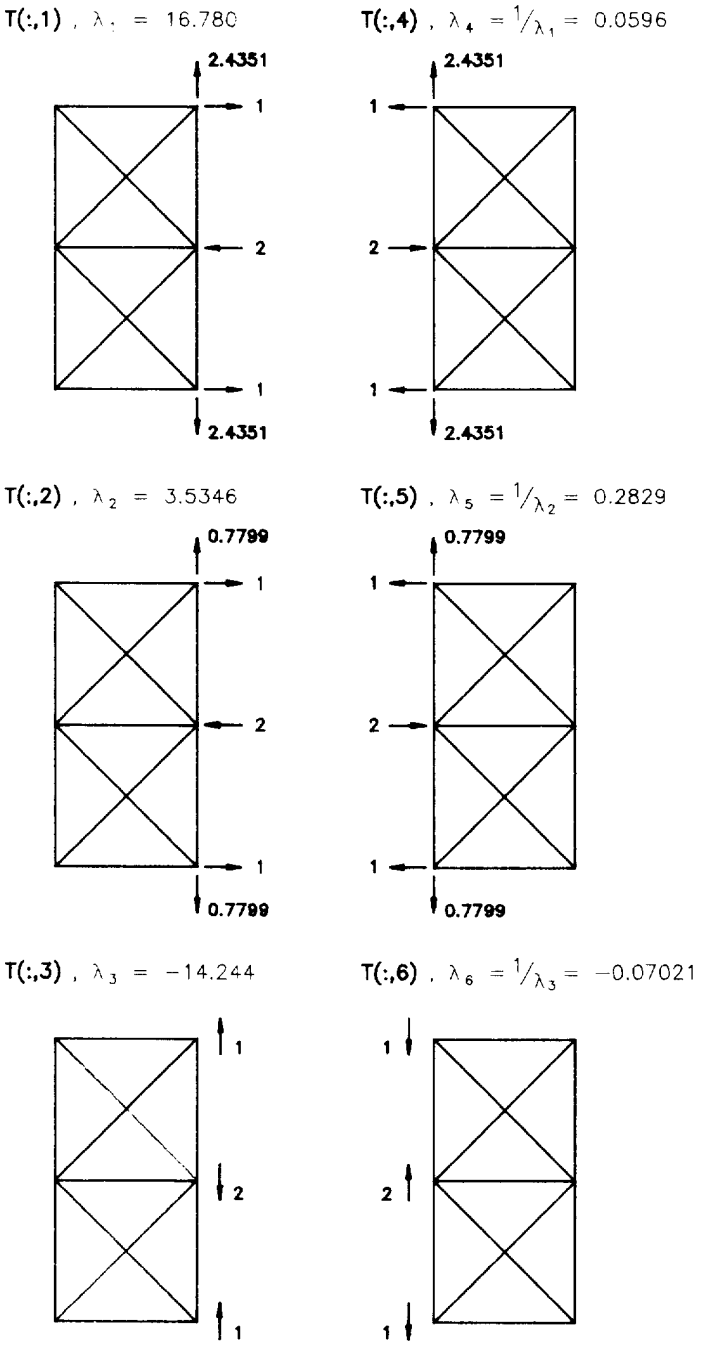

Fig. 10. Nodal forces for decay modes; displacements not shown.

$$\mathbf{GT}(:,10) = \mathbf{T}(:,10) + \mathbf{T}(:,9), \tag{19}$$

and this is shown physically in Fig. 12. Note that the expected y-component of displacement, due to cross-sectional rotation, in the vector $\mathbf{T}(:,10)$ is zero as the cosine of the angle of rotation is effectively unity.

The eleventh column, $\mathbf{T}(:,11)$, defines a bending moment on the cross-section of magnitude 2, and this is coupled with the tenth column according to the relationship

$$\mathbf{GT}(:,11) = \mathbf{T}(:,11) + \mathbf{T}(:,10), \tag{20}$$

as shown in Fig. 13.

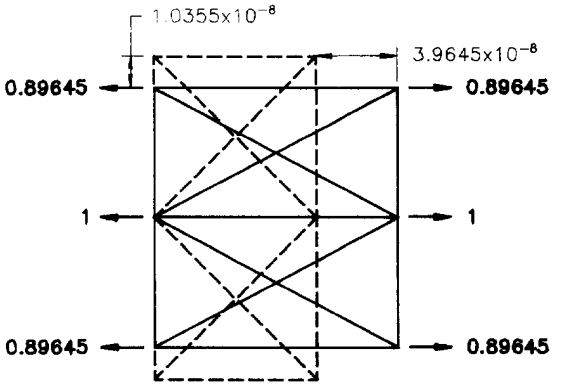

Fig. 11. Coupling of eigenvector T(:, 7) for rigid body displacement in the x-direction, with principal vector T(:, 8) for tension; displacements are exaggerated. Dotted lines show initial cell configuration.

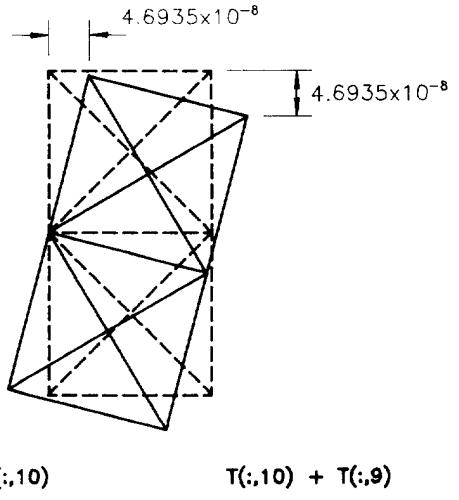

Fig. 12. Coupling of eigenvector T(:, 9) for rigid body displacement in the y-direction, with principal vector T(:, 10) for rotation; displacements in y-direction of left-hand face are negligible.

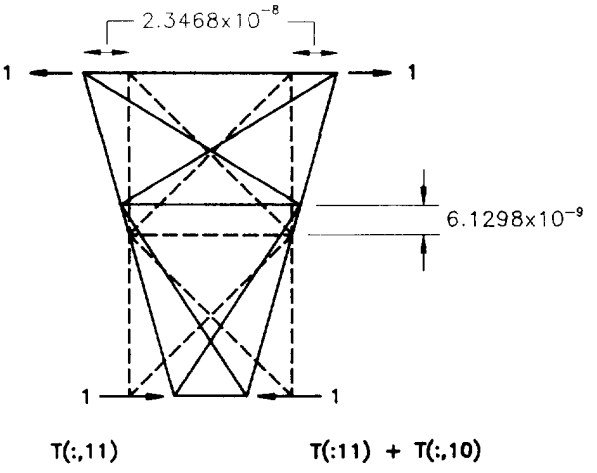

Fig. 13. Coupling of principal vector T(:, 10) for rotation, with principal vector for bending moment T(:, 11).

The constitutive relationship for beam bending is $M = EI/R$, where M is bending moment and R is beam curvature, and by geometric considerations we find that $1/R = 4.6935 \times 10^{-8}$; thus the equivalent second moment of area is found to be $I = 2.13061 \times 10^{-4}$ m^4.

Figure 13 also shows an apparent shift of the neutral axis towards the tension side of the cell; in fact this is a Poisson's ratio effect whereby during pure bending, transverse displacement of the upper and lower surfaces of the beam is greater than that of the neutral axis. Thus from Sokolnikoff (1956), article 32, the transverse displacement in the y-direction is (ignoring the constants of integration),

$$v = -\frac{M}{2EI}(x^2 + \nu y^2), \tag{21}$$

where a minus sign has been introduced to account for the different coordinate axes. Thus the transverse displacement at the neutral axis ($y = 0$) is

$$v_{y=0} = -\frac{M}{2EI}x^2 = 6.1298 \times 10^{-9}, \tag{22}$$

while the transverse displacement at the upper and lower surfaces ($y = \pm 1$) is zero, i.e.

$$v_{y=\pm 1} = -\frac{M}{2EI}(x^2 + \nu) = 0. \tag{23}$$

Combining these two results together with $M = 2$, $E = 200 \times 10^9$ N m^{-2}, $I = 2.13061 \times 10^{-4}$ m^4 again leads to Poisson's ratio $\nu = 0.2612$; it is gratifying that there should be no conflict between the two Poisson's ratio effects.

Finally, we consider the twelfth column $\mathbf{T}(:, 12)$ which defines a shearing force and a bending moment; this is coupled with the eleventh column $\mathbf{T}(:, 11)$ according to the relationship

$$\mathbf{GT}(:, 12) = \mathbf{T}(:, 12) + \mathbf{T}(:, 11), \tag{24}$$

and this is shown physically in Fig. 14.

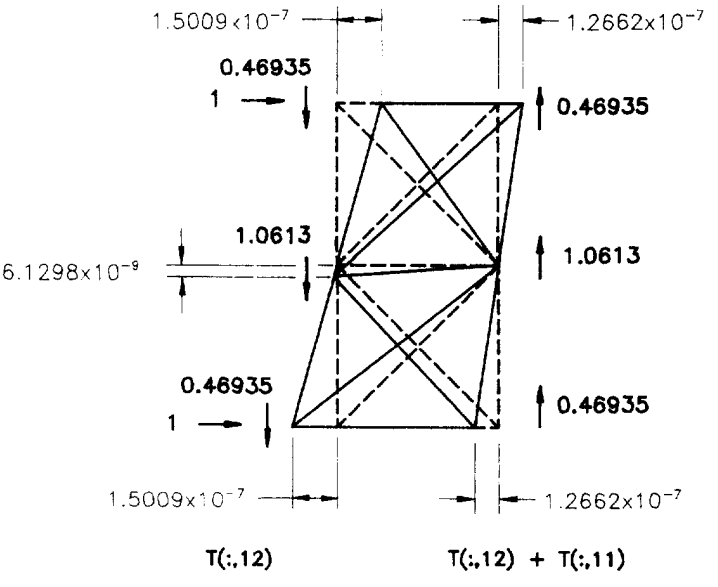

Fig. 14. Coupling of principal vector $\mathbf{T}(:, 12)$ for shearing force and bending moment, with principal vector $\mathbf{T}(:, 11)$ for bending moment.

We see that shearing forces of magnitude 2 on both cross-sections are balanced by a bending moment of magnitude 2 on the left-hand cross-section.

For a "one-dimensional" continuum beam the deflection due to shear is incorporated by the introduction of a shear coefficient κ within the equation

$$Q = \kappa AG\gamma, \tag{25}$$

where Q is the shearing force, A is the cross-sectional area, G is the shear modulus and γ is the shear angle; within Timoshenko beam theory (1921), the shear angle is defined according to the relationship

$$\gamma = \psi - \frac{\mathrm{d}v}{\mathrm{d}x}, \tag{26}$$

where $\mathrm{d}v/\mathrm{d}x$ is the centreline slope and ψ is rotation of the cross-section. The simplest method of evaluating the shear angle is to impose a rotation on the cell in Fig. 14 to bring the centreline slope to the horizontal, when $\mathrm{d}v/\mathrm{d}x$ is zero and $\gamma = \psi$; the cross-sectional rotations on either side of the cell are then different and taking the average gives a shear angle of $\gamma = 1.44486 \times 10^{-3}$. Employing $Q = 2$, equivalent shear modulus $G = E/2(1+\nu) = 79.29 \times 10^{9}$ N m^{-2} and equivalent area as calculated above, the equivalent shear coefficient is calculated as $\kappa = 0.4956$.

6. ANALYSIS OF HOFF'S THREE-DIMENSIONAL FRAMEWORK

We now return to Hoff's third framework; the transfer matrix† is now (24×24), and has 12 unity eigenvalues and the six reciprocal pairs of decay eigenvalues

$$\begin{bmatrix} 3.0744 + 2.1491i \\ 0.2185 - 0.1527i \end{bmatrix}, \begin{bmatrix} 3.0744 - 2.1491i \\ 0.2185 + 0.1527i \end{bmatrix}, \begin{bmatrix} -22.684 \\ -0.0441 \end{bmatrix}, \begin{bmatrix} -13.238 \\ -0.0755 \end{bmatrix}, \begin{bmatrix} -15.248 \\ -0.0656 \end{bmatrix}, \begin{bmatrix} -15.248 \\ -0.0656 \end{bmatrix}.$$

As before the unity eigenvalues are associated with rigid body displacements in the x-, y- and now the z-directions; coupled with these are rotations, tension, shear and bending in two planes, and torsion.

The decay eigenmodes show two new features: firstly there are now pairs of repeated real eigenvalues having independent eigenvectors, which is a consequence of the rotational symmetry of the framework; secondly there are now pairs of complex conjugate eigenvalues, having complex eigenvectors. It is noteworthy that the real eigenmodes self-equilibrate over each "chord" of the end of the framework, while the complex modes self-equilibrate over the end section of the framework as a whole.

As with the previous two-dimensional example, an applied end load may be expanded into its constituent modes by employing the bi-orthogonality property; in the present three-dimensional example the presence of complex eigenvectors deserves comment. Firstly, we note that a complex eigenvector is not physically permissible, but when considered in conjunction with its conjugate, the actual displacements and loads are the real and imaginary parts in turn. On the other hand, mathematically it is preferable to retain the complex eigenvector, in which case the modal expansion will lead to a pair of complex conjugate participation factors, γ_j. Additionally it must be remembered that the dot product of two complex vectors $\mathbf{a}$ and $\mathbf{b}$ is defined as $\mathbf{a} \cdot \mathbf{b} = \bar{\mathbf{a}}^{\mathrm{T}}\mathbf{b}$, where an overbar denotes the complex conjugate. To illustrate the procedure, and also the details for the repeated real eigenvalues, we consider Hoff's end load.

The free end load vector is

$$\mathbf{p}_0 = [0\,0\,-100\quad 0\,0\,0\quad 100\quad 0\,0\quad 0\quad -100\quad 0\,0\quad 0\quad 100]^{\mathrm{T}},$$

† For brevity the transfer matrix and eigenvectors and principal vectors are not listed in full.

and the associated displacement vector, according to the procedure described in Section 5, is

$$\mathbf{d}_0 = 10^{-6} \times [-a \quad -ab \quad -aa \quad -b \quad aab \quad a \quad -a \quad -b]^{\mathrm{T}},$$

where $a = 1.1209$, $b = 4.8251$.

Expanding the vector $\mathbf{s}_0$ as†

$$\mathbf{s}_0 = \sum_{i=1}^{12} \alpha_i \mathbf{X}_i, \tag{27}$$

and noting that eigenvectors $\mathbf{X}_1$, $\mathbf{X}_2$, $\mathbf{X}_7$ and $\mathbf{X}_8$ are complex, then

$$\alpha_1 = \frac{\mathbf{Y}_1 \cdot \mathbf{s}_0}{\mathbf{Y}_1 \cdot \mathbf{X}_1} = \frac{\bar{\mathbf{Y}}_1^{\mathrm{T}} \mathbf{s}_0}{\bar{\mathbf{Y}}_1^{\mathrm{T}} \mathbf{X}_1} = \frac{\mathbf{Y}_2^{\mathrm{T}} \mathbf{s}_0}{\mathbf{Y}_2^{\mathrm{T}} \mathbf{X}_1} = O(-8), \quad \alpha_2 = \bar{\alpha}_1.$$

Similarly, we find $\alpha_3 = O(-10)$, $\alpha_4 = O(-10)$. The eigenvalues λ_5 and λ_6 are identical, but the eigenvectors are independent, which leads to a "block" form for $\mathbf{Y}^{\mathrm{T}}\mathbf{X}$ when the coefficients α_5 and α_6 are obtained by solving

$$\begin{aligned} \alpha_5 \mathbf{Y}_5^{\mathrm{T}} \mathbf{X}_5 + \alpha_6 \mathbf{Y}_5^{\mathrm{T}} \mathbf{X}_6 &= \mathbf{Y}_5^{\mathrm{T}} \mathbf{s}_0 \\ \alpha_5 \mathbf{Y}_6^{\mathrm{T}} \mathbf{X}_5 + \alpha_6 \mathbf{Y}_6^{\mathrm{T}} \mathbf{X}_6 &= \mathbf{Y}_6^{\mathrm{T}} \mathbf{s}_0 \end{aligned} \tag{28}$$

from which $\alpha_5 = O(-9)$, $\alpha_6 = O(-11)$. The coefficients α_9, α_{10}, α_{11} and α_{12} are found in identical fashion, and are of similar order. The remaining coefficients are straightforward to determine, the only significant ones being $\alpha_7 = 50 - 48.263\mathrm{i}$, $\alpha_8 = 50 + 48.263\mathrm{i}$. Thus the applied end load may be expanded as

$$\mathbf{s}_0 = \alpha_7 \mathbf{X}_7 + \alpha_8 \mathbf{X}_8 = \alpha_7 \mathbf{X}_7 + \bar{\alpha}_7 \bar{\mathbf{X}}_7 \tag{29}$$

and nodal forces on the nth section may be determined from the equation

$$\mathbf{s}_n = (50 - 48.263\mathrm{i})\mathbf{X}_7(0.2185 + 0.1527\mathrm{i})^n + (50 + 48.263\mathrm{i})\bar{\mathbf{X}}_7(0.2185 - 0.1527\mathrm{i})^n. \tag{30}$$

where

$$\mathbf{X}_7 = [p \; p \; q \quad p \; -p \quad -q \quad -p \; -p \; q \quad -p \; p \; -q \quad c \; c \; -d \quad c \; -c \; d \quad -c \; -c \; -d \quad -c \; c \; d]^{\mathrm{T}}$$

and $p = (2.2855 - 3.5290\mathrm{i}) \times 10^{-5}$, $q = (3.6626 + 1.2044\mathrm{i}) \times 10^{-5}$, $c = -0.5186$, $d = 1.0$.

7. CONCLUDING REMARKS

By employing the transfer matrix of a single cell to relate the state variables on either side, the calculation of equivalent beam properties and decay modes for a pin-jointed framework of repeating cells is reduced to standard eigen analysis, thus providing a very efficient means of determining both. The procedure described here is capable of extension to rigid joints at the expense of an increase in dimension of the state vector and transfer matrix, since a rigid joint implies an additional bending moment and rotation *at each node*. For a two-dimensional framework the state vector would increase in size by 50%, while a three-dimensional framework would imply bending moments in two planes, together with the associated bending rotations, and a twisting moment and rotation; each node therefore requires six force or moment components and six displacement components, and the state vector for a section would have 48 components, an increase of 100%.

The procedure has also been developed for determination of the decay eigenmodes of a

† Since the end load of Fig. 4 is clearly self-equilibrating, it is expanded in terms of the (first) 12 decay eigenmodes; the remaining 12 eigenmodes pertain to the rigid body displacements and the transmitting modes.

continuum beam, for which exact analytical solutions are available only for mathematically amenable cross-sections such as the circle or the plane strain strip, as an extension of the finite element method; the authors describe this application to beams of general cross-section in a separate report.

Acknowledgement The authors give special thanks to R. J. Dooler of the Central Design Service at Southampton University for preparation of the drawings.

REFERENCES

Hoff, N. J. (1945). The applicability of Saint-Venant's principle to airplane structures. *J. Aeronautical Sci.* **12,** 455–460.

Horgan, C. O. (1989). Recent developments concerning Saint-Venant's principle: an update. *ASME Appl. Mech. Rev.* **42,** 295–303.

Horgan, C. O. and Knowles, J. K. (1983). Recent developments concerning Saint-Venant's principle. In *Advances in Applied Mechanics* (Edited by J. W. Hutchinson), Vol. 23, 79–269. Academic Press, New York.

Noor, A. K. (1988). Continuum modeling for repetitive lattice structures. *Appl. Mech. Rev.* **41,** 285–296.

Noor, A. K., Anderson, C. M. and Green, W. H. (1978). Continuum models for beam- and platelike lattice structures. *AIAA J.* **16,** 1219–1228.

Noor, A. K. and Nemeth, M. P. (1980). Micropolar beam models for lattice grids with rigid joints. *Comput. Meth. Appl. Mech. Engng* **21,** 249–263.

Przemieniecki, J. S. (1968). *Theory of Matrix Structural Analysis*. McGraw-Hill, New York.

Renton, J. D. (1984). The beam-like behaviour of space trusses. *AIAA J* **22,** 273–280.

Sokolnikoff, I. S. (1956). *Mathematical Theory of Elasticity*. McGraw-Hill, New York.

Stasa, F. L. (1985). *Applied Finite Element Analysis for Engineers*. Holt, Rinehart and Winston, New York.

Timoshenko, S. P. (1921). On the correction for shear for the differential equation for transverse vibrations of prismatic bars. *Phil. Mag. Series* 6, **41,** 744–746.

Toupin, R. A. (1965). Saint-Venant's Principle. *Arch. Rat. Mech. Anal.* **18,** 83–96.

Vlasov, V. V. (1961). *Thin Walled Elastic Beams*. The Israel Program For Scientific Translation.

APPENDIX

$$\mathbf{T} = \begin{bmatrix} 1.6410\times10^{-8} & 4.2911\times10^{-8} & -6.1298\times10^{-9} & -1.6410\times10^{-8} & -4.2911\times10^{-8} & -6.1298\times10^{-9} \\ 1.7438\times10^{-7} & 3.9532\times10^{-8} & 4.6103\times10^{-8} & 1.7438\times10^{-7} & 3.9532\times10^{-8} & -4.6103\times10^{-8} \\ -7.9855\times10^{-8} & -9.3087\times10^{-8} & 0 & 7.9855\times10^{-8} & 9.3087\times10^{-8} & 0 \\ 0 & 0 & -4.0777\times10^{-8} & 0 & 0 & 4.0777\times10^{-8} \\ 1.6410\times10^{-8} & 4.2911\times10^{-8} & 6.1298\times10^{-9} & -1.6410\times10^{-8} & -4.2911\times10^{-8} & 6.1298\times10^{-9} \\ -1.7438\times10^{-7} & -3.9532\times10^{-8} & 4.6103\times10^{-8} & -1.7438\times10^{-7} & -3.9532\times10^{-8} & -4.6103\times10^{-8} \\ 1 & 1 & 0 & 1 & 1 & 0 \\ 2.4351 & 7.7990\times10^{-1} & 1 & -2.4351 & -7.7990\times10^{-1} & 1 \\ -2 & -2 & 0 & -2 & -2 & 0 \\ 0 & 0 & -2 & 0 & 0 & -2 \\ 1 & 1 & 0 & 1 & 1 & 0 \\ -2.4351 & -7.7990\times10^{-1} & 1 & 2.4351 & 7.7990\times10^{-1} & 1 \end{bmatrix}$$

$$\begin{bmatrix} 3.9645\times10^{-8} & 0 & 0 & 4.6935\times10^{-8} & -2.3468\times10^{-8} & 1.5009\times10^{-7} \\ 0 & -1.0355\times10^{-8} & -4.6935\times10^{-8} & 0 & 0 & 0 \\ 3.9645\times10^{-8} & 0 & 0 & 0 & 0 & 0 \\ 0 & 0 & -4.6935\times10^{-8} & 0 & 6.1298\times10^{-9} & -6.1298\times10^{-9} \\ 3.9645\times10^{-8} & 0 & 0 & -4.6935\times10^{-8} & 2.3468\times10^{-8} & -1.5009\times10^{-7} \\ 0 & 1.0355\times10^{-8} & -4.6935\times10^{-8} & 0 & 0 & 0 \\ 0 & 8.9645\times10^{-1} & 0 & 0 & 1 & -1 \\ 0 & 0 & 0 & 0 & 0 & 4.6935\times10^{-1} \\ 0 & 1 & 0 & 0 & 0 & 0 \\ 0 & 0 & 0 & 0 & 0 & 1.0613 \\ 0 & 8.9645\times10^{-1} & 0 & 0 & -1 & 1 \\ 0 & 0 & 0 & 0 & 0 & 4.6935\times10^{-1} \end{bmatrix}$$

$\mathbf{T}^{-1}\mathbf{G}\mathbf{T} = \mathbf{J}$, where $\mathbf{J}$ is a Jordan block matrix,

$$\mathbf{J} = \left[\begin{array}{cccccc|cccccc}
1.6780\times10^{1} & 0 & 0 & 0 & 0 & 0 & & & & & & \\
0 & 3.5346 & 0 & 0 & 0 & 0 & & & & & & \\
0 & 0 & -1.4244\times10^{1} & 0 & 0 & 0 & & & & & & \\
0 & 0 & 0 & 5.9596\times10^{-2} & 0 & 0 & & & & & & \\
0 & 0 & 0 & 0 & 2.8292\times10^{-1} & 0 & & & & & & \\
0 & 0 & 0 & 0 & 0 & -7.0207\times10^{-2} & & & & & & \\
\hline
0 & 0 & 0 & 0 & 0 & 0 & & & & & & \\
0 & 0 & 0 & 0 & 0 & 0 & & & & & & \\
0 & 0 & 0 & 0 & 0 & 0 & & & & & & \\
0 & 0 & 0 & 0 & 0 & 0 & & & & & & \\
0 & 0 & 0 & 0 & 0 & 0 & & & & & & \\
0 & 0 & 0 & 0 & 0 & 0 & & & & & &
\end{array}\right.$$

$$\left.\begin{array}{cc|cccc}
0 & 0 & 0 & 0 & 0 & 0 \\
0 & 0 & 0 & 0 & 0 & 0 \\
0 & 0 & 0 & 0 & 0 & 0 \\
0 & 0 & 0 & 0 & 0 & 0 \\
0 & 0 & 0 & 0 & 0 & 0 \\
0 & 0 & 0 & 0 & 0 & 0 \\
\hline
1 & 1 & 0 & 0 & 0 & 0 \\
0 & 1 & 0 & 0 & 0 & 0 \\
\hline
0 & 0 & 1 & 1 & 0 & 0 \\
0 & 0 & 0 & 1 & 1 & 0 \\
0 & 0 & 0 & 0 & 1 & 1 \\
0 & 0 & 0 & 0 & 0 & 1
\end{array}\right].$$